ORIGINAL ARTICLE

Shell Biosynthesis and Pigmentation as Revealed by the Expression of Tyrosinase and Tyrosinase-like Protein Genes in Pacific Oyster (*Crassostrea gigas*) with Different Shell Colors

Yijing Zhu[1] · Qi Li[1,2] · Hong Yu[1] · Shikai Liu[1] · Lingfeng Kong[1]

Abstract

The widely recognized color polymorphisms of molluscan shell have been appreciated for hundreds of years by collectors and scientists, while molecular mechanisms underlying shell pigmentation are still poorly understood. Tyrosinase is a key rate–limiting enzyme for the biosynthesis of melanin. Here, we performed an extensive multi-omics data mining and identified two tyrosinase genes, including tyrosinase and tyrosinase-like protein 2 (*Tyr* and *Typ-2* respectively), in the Pacific oyster *Crassostrea gigas*, and investigated the expression patterns of tyrosinase during adults and embryogenesis in black and white shell color *C. gigas*. Tissue expression analysis showed that two tyrosinase genes were both specifically expressed in the mantle, and the expression levels of *Tyr* and *Typ-2* in the edge mantle were significantly higher than that in the central mantle. Besides, *Tyr* and *Typ-2* genes were black shell-specific compared with white shell oysters. In situ hybridization showed that strong signals for *Tyr* were detected in the inner surface of the outer fold, whereas positive signals for *Typ-2* were mainly localized in the outer surface of the outer fold. In the embryos and larvae, the high expression of *Tyr* mRNA was detected in eyed-larvae, while *Typ-2* mRNA was mainly expressed at the trochophore and early D-veliger. Furthermore, the tyrosinase activity in the edge mantle was significantly higher than that in the central mantle. These findings indicated that *Tyr* gene may be involved in shell pigmentation, and *Typ-2* is more likely to play critical roles not only in the formation of shell prismatic layer but also in shell pigmentation. In particular, *Typ-2* gene was likely to involve in the initial non-calcified shell of trochophores. The work provides valuable information for the molecular mechanism study of shell formation and pigmentation in *C. gigas*.

Keywords *Tyr* · *Typ-2* · *Crassostrea gigas* · Pigmentation · Biosynthesis

Abbreviations

Tyr	A member of the type-3 copper protein superfamily
Typ-2	Tyrosinase-like protein 2

✉ Qi Li
qili66@ouc.edu.cn

1   Key Laboratory of Mariculture, Ministry of Education, Ocean University of China, Qingdao 266003, China

2   Laboratory for Marine Fisheries Science and Food Production Processes, Qingdao National Laboratory for Marine Science and Technology, Qingdao 266237, China

Introduction

The fabulous and diverse surface color of aquatic animals, as the most intuitive phenotypic trait, is one of the factors influencing consumers' preference and price at the seafood market (Alfnes et al. 2006). The widespread color polymorphisms of a molluscan shell have always been appreciated by collectors and a great deal of scientists. However, shell formation and pigmentation have not been completely elucidated for any mollusk compared with plants, vertebrates, and certain invertebrate groups (Williams et al. 2017). Although shell color can be affected by biochemistry, substrate or nutrition (Liu et al. 2009; Zhu et al. 2018), breeding studies in both bivalves and gastropods have shown that color polymorphism in many species is a heritable trait, and in some cases, inheritance patterns involve one or two loci with dominance (Yusa 2004; Xu et al. 2019; Han and Li 2020).

Recently, a large amount of transcriptomic, proteomic, and genomic data in terms of the shell formation and pigmentation have been generated in mollusca (Feng et al. 2015; McDougall and Degnan 2018). Some potential genes have been identified that may have some control over shell pigmentation, although in most studies it is not possible to rule out that some of these genes may rather be involved in biomineralization (Jackson et al. 2006; Lemer et al. 2015). A study on *Pinctada margaritifera* suggested that the color of the nacre is partially under the influence of genes involved in the biomineralization of the calcitic layer (Lemer et al. 2015). These studies provide useful resource for molecular and genetic analyses of shell formation and pigmentation.

Much of the pigment-based coloration in mollusca results from products of the melanin, carotenoid, and tetrapyrrole synthesis pathways to date (Williams 2017). Of them, melanin is the most widespread pigment in nature. In mollusks, melanin is secreted from the epithelium of the mantle edge and in the pallial area (Jabbour-Zahab et al. 1992). Although the complete pathways involved in the synthesis of melanin are unknown, several enzymes have been shown to be important in the regulation and production of melanin in mollusks (Palumbo 2003; Lemer et al. 2015). Arguably, one of the most important enzymes is tyrosinase.

Tyrosinase is a member of the type-3 copper protein superfamily and has two conserved copper-binding domains, Cu (A) and Cu (B) (Ren et al. 2020). High-level activities of tyrosinase are positively correlated to the production of melanin due to the fact that tyrosinase was reported to be an important rate-limiting enzyme in melanin synthesis (Hoekstra 2006; Gutierrez-Gil et al. 2007). Tyrosinase activity from shellfish has been found in hemocytes (Luna-González et al. 2003), eggs (Bai et al. 1997), and the mantle (Chen et al. 2017). In a few mollusks, tyrosinase was considered to play a key role not only in melanin synthesis but also in the formation of shell matrix and pigmentation of prismatic layer (Nagai et al. 2007; Takgi and Miyashita 2014; Chen et al. 2017). A recent study on *Pteria penguin* indicated that tyrosinase was responsible for melanin synthesis and color formation (Yu et al. 2018). Chen et al. (2017) found that HcTyr and HcTyp-1 may be involved in the formation of nacre color in *Hyriopsis cumingii.* Conversely, several genes associated with melanin synthesis were identified in *P. margaritifera*, and the gene ZINC (a homolog of tyrosinase-related protein 1) was upregulated in the full albino shells but downregulated in normal black and half-albino specimens (Lemer et al. 2015).

The Pacific oyster (*Crassostrea gigas*), as a representative bivalve species which has been the most widely farmed in the world, is a potential model for marine mollusca studies owing to its economic and ecological importance plus suitable biological characteristics (Yu et al. 2016). In our selective breeding practice of the Pacific

oyster, four shell color strains (golden, white, black, and orange) of the Pacific oyster were successfully developed. Transcriptomic data of different shell color *C. gigas* showed that at 12 transcripts coding for tyrosinase-related genes existed in the mantle, implying that the expansion of this gene family has occurred during the evolution of this species (Feng et al. 2015). Recently, knockdown *CgTyr* using the bacteria-expressing dsRNA stratege could block the shell growth and color formation in the Pacific oysters, indicating that tyrosinase plays a vital role in the assembly and maturation of shell matrices (Feng et al. 2019). Huan et al. (2013) speculated that a tyrosinase gene might function in the initial phase of the larval shell biogenesis in the normal *C. gigas*. However, whether tyrosinase acted as an important regulator to control the melanin biosynthesis and adult shell formation in the Pacific oyster is poorly studied. In addition, it remains unclear whether these genes play an essential role in larval shell pigmentation and developments in the black shell *C. gigas*.

In this study, we performed a multi-omics data mining and identified two tyrosinase genes, including tyrosinase (*Tyr*) LOC_105324827 and tyrosinase-like protein 2 (*Typ-2*) LOC_105344040 in the Pacific oyster genome. We further utilized the selectively breed variety of *C. gigas* with black shell and white shell as research models to investigate potential involvement of the two genes in shell construction and pigment production in order to provide valuable information on genetic bases directly linked to shell biosynthesis and pigmentation in the oyster.

Materials and Methods

Sequence Analysis

The amino acid sequences of tyrosinase/tyrosinase-like protein from *Mus musculus*, *Danio rerio*, *Sepia officinalis*, *Hyriopsis cumingii*, *Mizuhopecten yessoensis*, *Azumapecten farreri*, *Meretrix meretrix*, *Pinctada margaritifera*, *Pinctada imbricata*, *Pinctada fucata*, *Crassostrea virginica* and *Crassostrea gigas* were retrieved from the NCBI database followed by further manual curation and phylogenetic analysis. Sequence alignment of the domains was performed using the DNAMAN version 8.0 (Lynnon BioSoft, USA). Signal 4.1 program (http://www.cbs.dtu.dk/services/SignalP/) was used to predict signal peptide of *Tyr*. The protein structural domains were further predicted using the online research tool (SMART, http://smart.embl-heidelberg.de/) (Letunic et al. 2015). Phylogenetic tree was constructed using MEGA 7.0 (Kumar et al. 2016) based on the neighbor-joining (NJ) method with 2000 bootstrap replicates.

Animals and Sampling

Nine-month-old Pacific oysters with a black shell and white shell were collected from the culture population in Weihai, Shandong, China (Fig. 1A). The left mantle was fixed in 4% paraformaldehyde (PFA) in 0.1 M phosphate-buffered saline (PBS) overnight at 4 °C for in situ hybridization (ISH). The anterior side and posterior side of the edge and central mantles of both the left and right sides (AEML, AEMR, PEML, PEMR, CML, CMR; Fig. 1B) were sampled, flash-frozen in liquid nitrogen and stored at −80 °C prior to RNA extraction. The other adult tissues including gill, adductor muscle, labial palps, gonad, and hemolymph were sampled from oysters, also frozen in liquid nitrogen and stored at −80 °C.

Embryonic and larval samples were obtained and cultured according to Wang et al. (2012). Unfertilized oocytes, 2-cell, 4-cell, 8-cell, morula, blastula, and gastrula embryos, and trochophores, D-veliger larvae, umbo-larvae, and eyed-larvae were sampled and treated the same as mantle-tissue procedure.

RNA Extraction and cDNA Preparation

Total RNAs were extracted from adult tissues and embryonic–larval samples using a Trizol reagent

Fig. 1 The shell pictures (**A**) and different mantle regions (**B**) of the Pacific oyster *Crassostrea gigas*
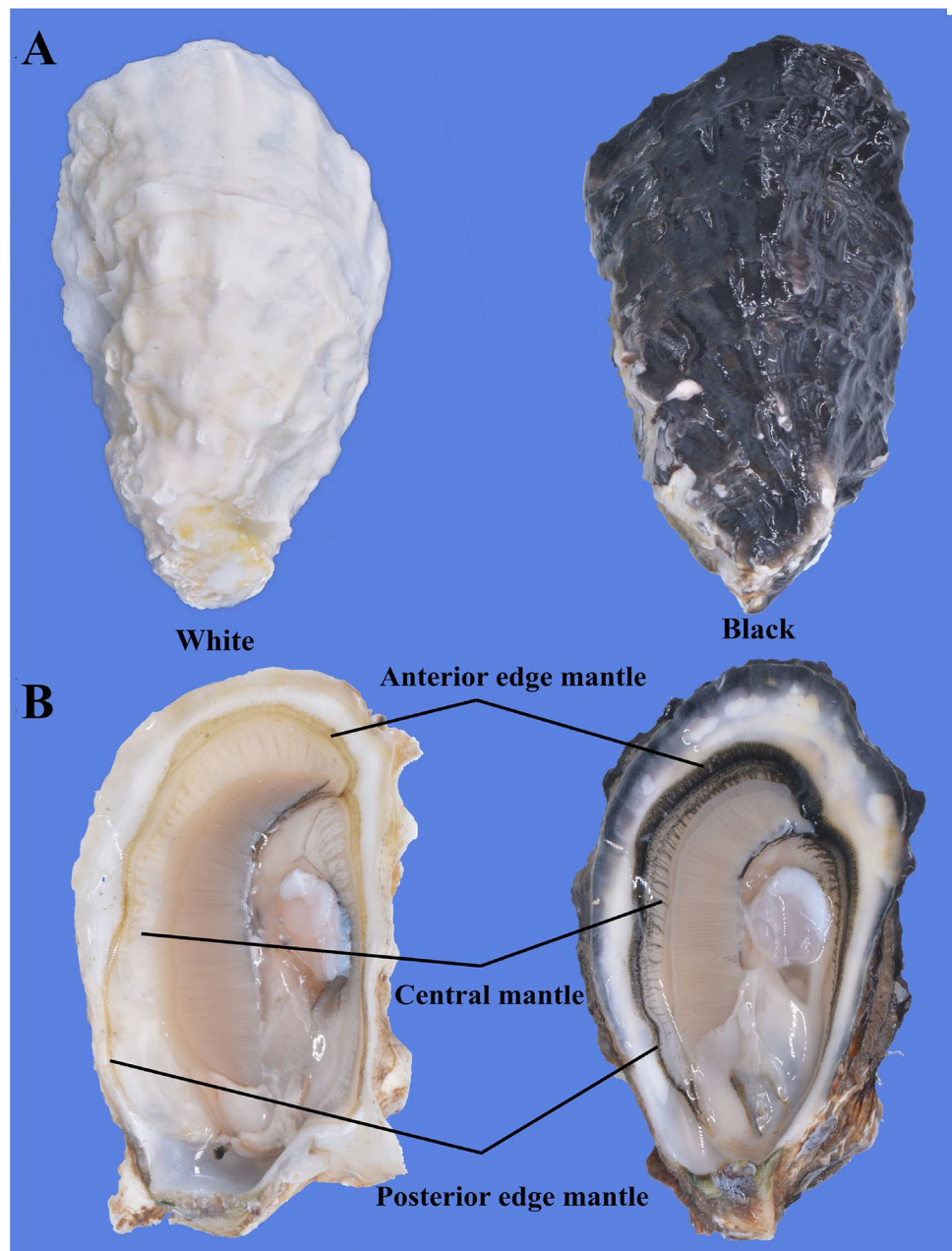
(Invitrogen) according to the manufacturer's protocols. RNA concentrations, integrity, and quality were verified by NanoDrop 2000 (Thermo Scientific) and gel electrophoresis. For gene expression analysis, total RNAs (1000 ng) extracted from each sample were reversely transcribed into cDNA according to the PrimeScriptTM reverse transcription kit with gDNA Eraser (Perfect Real Time) (TaKaRa, Japan) strictly following the manufacturer's instructions.

Real-time PCR Analysis

Real-time PCR was used to measure the tyrosinase gene expression level in the *C. gigas*. The primer sets used for real-time PCR were designed using Primer Premier 5 software (Table 1). PCR reactions were cycled 40 amplification cycles (5 s/95 °C, 20 s/60 °C, 20 s/72 °C) using EvaGreen $2 \times$ qPCR MasterMix-ROX (ABM) on a LightCycler® 480 real-time PCR machine (Roche, Switzerland) in a 10-µL reaction. Parallel amplifications of elongation factor 1α (EF1α) reference gene were carried out in the adult and larval *C. gigas* (Xu et al. 2018). Melting curves were used for each individual amplicon to ensure the accurate amplification. Relative expression levels of the target gene were calculated as $2^{-\Delta\Delta CT}$.

Tissue In Situ Hybridization

Sense and antisense probe digoxigenin–labeled RNA strands were transcribed in vitro with a DIG RNA labeling Kit (Roche, Germany), and forward and reverse primers were tagged with a T7 promoter, respectively. Serial sections of 5 µm were produced on a Leica RM 2016 microtome (Leica, Germany). Sections were deparaffinized, hydrated, and treated with 10-µg/mL proteinase K for 10 min at 37 °C, and then prehybridized in the hybridization buffer for 4 h at 60 °C. Following this, sections were hybridized with sense and antisense probes for 16 h at 60 °C. After that, antibody incubation was performed with 1/5000 anti-DIG antibody (Roche, Switzerland) in 1% blocking reagents overnight at 4 °C. Hybridization signals were then detected using the NBT–BCIP mix (Roche, Switzerland) as the chromogen. Finally, sections were counterstained with 0.5% eosin and examined by an Olympus BX53 microscope.

Whole-mount In Situ Hybridization

Embryos fixed in 4% paraformaldehyde were washed three times in methanol and stored at −20 °C until use. Briefly, the embryos were rehydrated to PBST through graded methanol baths, then treated with an age-dependent concentration of proteinase K (50 ng–5 µg/mL) for 30 min at 37 °C. Following this, the samples were treated in the same way as the tissue samples stated above.

Analysis of the Tyrosinase Activity

The tyrosinase activity was determined using the tissue tyrosinase activity assay kit (Solarbio, Beijing, China) according to the manufacturer's instructions. In brief, the fresh edge and central mantles (1 g) of left side were sampled from the black and white shells. Then, the mantles were homogenized with a homogenizer and treated with the lysis buffer. The solution was centrifuged for 20 min at 4 °C, and then, the supernatant was collected and then mixed with buffer and substrate (tyrosine). Finally, the samples were incubated at 25 °C for 50 min, and tyrosinase activity was measured using a spectrophotometer at 475 nm at room temperature (UV-2800A; Unico, Shanghai). One unit of tyrosinase activity was defined as the amount of activity that produced 1 nmol of dopachrome per minute via the hydroxylation of tyrosine by the standard tyrosinase at 25 °C and expressed as nmol/g wet weight.

Table 1 List of primer sequences used in this study

Primer names	Primer sequences (5′–3′)	Experiment
CgTyr-F	GGAGCAGCGTATTTCTTCACC	qRT–PCR
CgTyr-R	TTTGTCTTTGCCTTTGTCGG	qRT–PCR
CgTyp-2-F	GACTACTGACAGCGAGATGATGG	qRT–PCR
CgTyp-2-R	GAATCTTCCAAAGGGTCCAGTC	qRT–PCR
EF1α-F	AGTCACCAAGGCTGCACAGAAAG	qRT–PCR
EF1α-R	TCCGACGTATTTCTTTGCGATGT	qRT–PCR
CgTyr-F	CGAAACCAAGAGGATAGATTAGG	ISH
CgTyr-R	GATCACTAATACGACTCACTATAGGGCAACCAGATTGTATGAAGACAGACT	ISH
CgTyp-2-F	AGAGAGGGATTACCCAAGAGGAGT	ISH
CgTyp-2-R	GATCACTAATACGACTCACTATAGGGACTGAACGAAAACCTTTGCTGC	ISH

Statistical Analysis

Data from the qPCR experiments ($n = 9$) and tyrosinase activity experiments ($n=5$) were expressed as the mean ± SD. One-way ANOVA was performed using SPSS 21.0 with the significance level $P < 0.05$ to determine whether there were any significant differences.

Results

Sequence Analysis of *Tyr* and *Typ-2* in *C. gigas*

Two tyrosinase genes were identified in *C. gigas*, including tyrosinase (*Tyr*) and tyrosinase-like protein 2 (*Typ-2*). Amino acid sequence alignments of *Tyr* and *Typ-2* gene from *C. gigas* and other bivalves were performed. The *C. gigas Tyr* shared the highest (58.89%) identity with tyrosinase-like protein 1 of *C. virginica*, 32.55% with tyrosinase-like protein 2 of *M. yessoensis*. The *C. gigas Typ-2* showed 43% identity to *C. virginica* tyrosinase-like protein 1, and 32.55% to *M. yessoensis* tyrosinase-like protein 2. Amino acid sequence comparison revealed a conserved copper–binding domain Cu (A) and Cu (B), in which six histidine residues were highly conserved (Fig. 2A). *Tyr* and *Typ-2* encoded polypeptides that contained 699 and 658 amino acids, respectively (Fig. 2B). Further analysis of the signal peptide revealed that *C. gigas Tyr* and *Typ-2* possessed a transmembrane region in addition to a conserved CuA/CuB domain (Fig. 2B).

The different species of phylogenetic tree analysis was carried out to indicate the evolutionary relationships of tyrosinases. As shown in Fig. 2C, *Tyr* is close to tyrosinase-like protein 1 of *C. virginica* with a support of 100%, which belongs to the same clade. *Typ-2* was close to *C. gigas Tyr* and tyrosinase-like protein 1 of *C. virginica* with a support of 99%. All tyrosinases of shellfish referred, including *C. gigas*, were grouped into a close cluster, but some species showed a low support. The tyrosinases from *D. rerio* and *M. musculus* were classified to a vertebrate clade.

Expression Profiles of the Tyrosinases in Tissues of *C. gigas*

The expression patterns of *Tyr* and *Typ-2* in tissues of black shell *C. gigas* were analyzed by RT-qPCR. Significantly high expression levels of *Tyr* and *Typ-2* mRNA were detected in the mantle (Fig. 3). Whereas *Tyr* and *Typ-2* were expressed only at low or very low levels in other tissues. To investigate the role of the tyrosinase genes in the formation of shell color, the expression of *Tyr* and *Typ-2* in different mantle regions (edge and central mantles of the left and right sides) was first analyzed in black-shell oysters. As shown in Fig. 4,

the expression profiles of the two tyrosinase genes in different mantle regions shared a similar pattern. Both of the two genes were expressed at a higher level in the edge mantle (either in the anterior or posterior areas) compared with that in the central mantle either on the left or right sides. Interestingly, the higher expression level of the *Tyr* was detected in the anterior area of the left-edge mantle than that in the right-edge mantle (Fig. 4A). On the contrary, that of the *Typ-2* was dominantly expressed in the anterior side of the right edge (Fig. 4B).

With the central mantle expressing lower levels of tyrosinase, only the anterior side of left-edge mantle was used to compare the relative expression levels between the black and white shell colors. The patterns of expression levels of each of these two genes were similar between the two shell colors in terms of mantle edger, in which *Tyr* and *Typ-2* genes were expressed at significantly higher levels in the black shell than white shell oysters (Fig. 5).

Expression Profiles of the Tyrosinases in *C. gigas* During Embryonic–Larval Developmental Stages

The expression patterns of tyrosinase genes during embryonic and larval stages of black shell *C. gigas* were also analyzed by quantitative RT-PCR analysis. The *Tyr* mRNA was highly expressed in eyed-larvae, but was almost undetectable in other stages (Fig. 6A). By contrast, *Typ-2* mRNA was mainly expressed at the trochophore and early D-veliger (18 h) stages and was particularly high in the trochophore (Fig. 6B). With the larval development, the expression level of *Typ-2* rapidly decreased in the following developmental stages from D-veliger to eyed-larvae.

Localization of the Tyrosinases mRNA in *C. gigas* Mantle

ISH analysis showed that the two tyrosinase genes exhibited distinct expression patterns, which was generally consistent with the real-time PCR results. Positive signals of *Tyr* and *Typ-2* were found abundantly in the edge mantle, while no positive signal was detected in the central mantle (Figs. 7 and 8). The edge mantle was characterized by the enlargement of the sheath at the shell margin into three terminal folds: the outer fold (of), middle fold (mf), and the inner fold (if). Apparently, ISH analysis displayed strong signals for *Tyr* in the inner surface of the outer fold either in the black shell or white shell colors (Fig. 7). Conversely, the localization of *Typ-2* was detected in the outer surface of the outer fold, but not in the inner surface, which was different from the observation in *Tyr*. In contrast, no positive signals were detected when using the sense probes (data not shown).
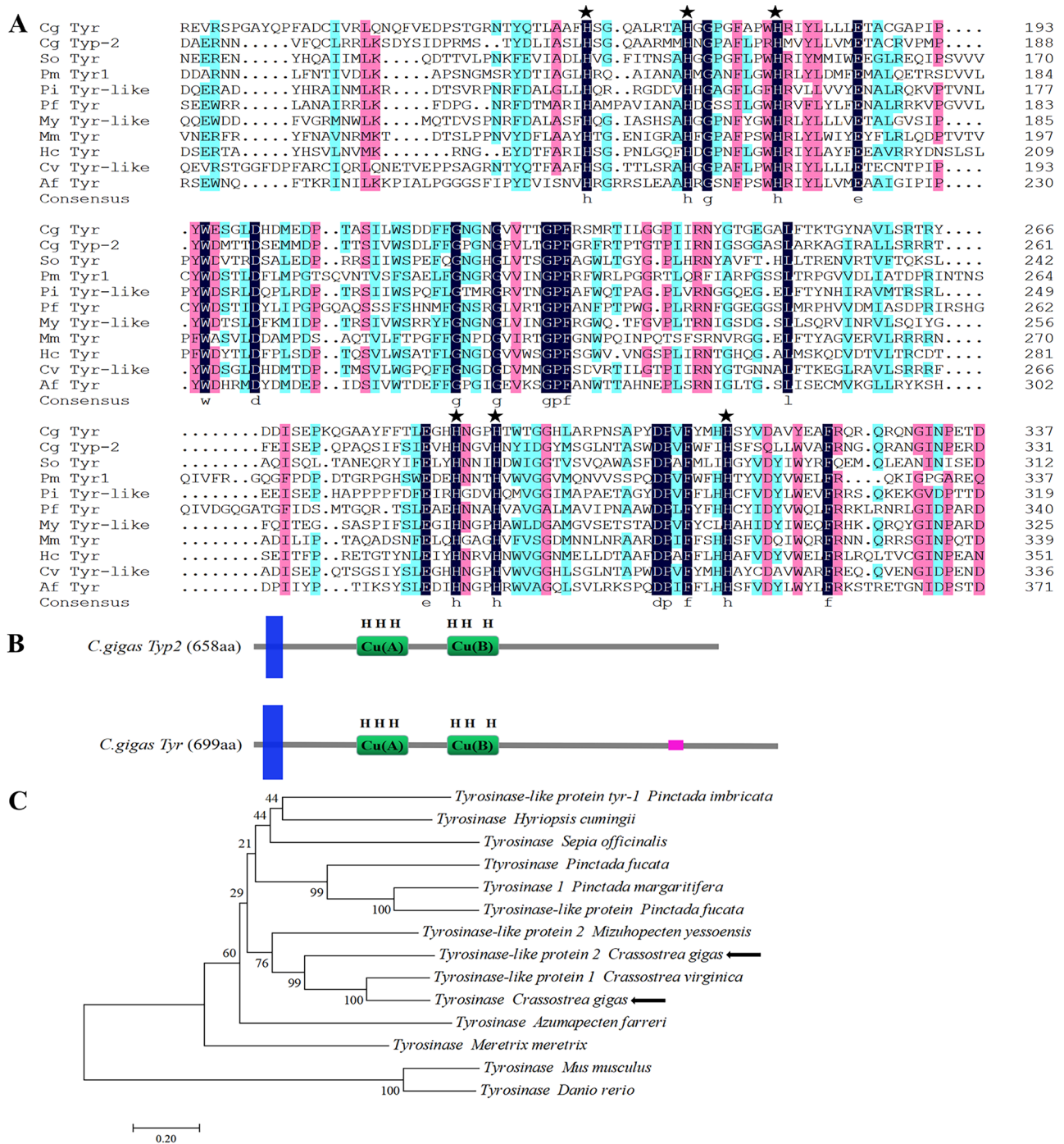
Fig. 2 Sequence alignment and phylogenetic analysis. **A**: Multiple sequence comparison of *Tyr* copper–binding domain among molluscans. Cg, *Crassostrea gigas*; So, *Sepia officinalis*; Pm, *Pinctada margaritifera*; Pi, *Pinctada imbricata*; Pf, *Pinctada fucata*; My, *Mizuhopecten yessoensis*; Mm, *Meretrix meretrix*; Hc, *Hyriopsis cumingii*; Cv, *Crassostrea virginica*; Af, *Azumapecten farreri*. The conserved amino acids were written in black background, and similar amino acids were shaded in green and pink. The highly conserved histidine residues were signed with ★. **B**: Schemes depicting the structure of *Tyr* and *Typ-2* protein in *C. gigas*. The Cu (A)/Cu (B) domain with six conserved histidine residues was shown in green box. **C**: Phylogenetic analyses of tyrosinase genes
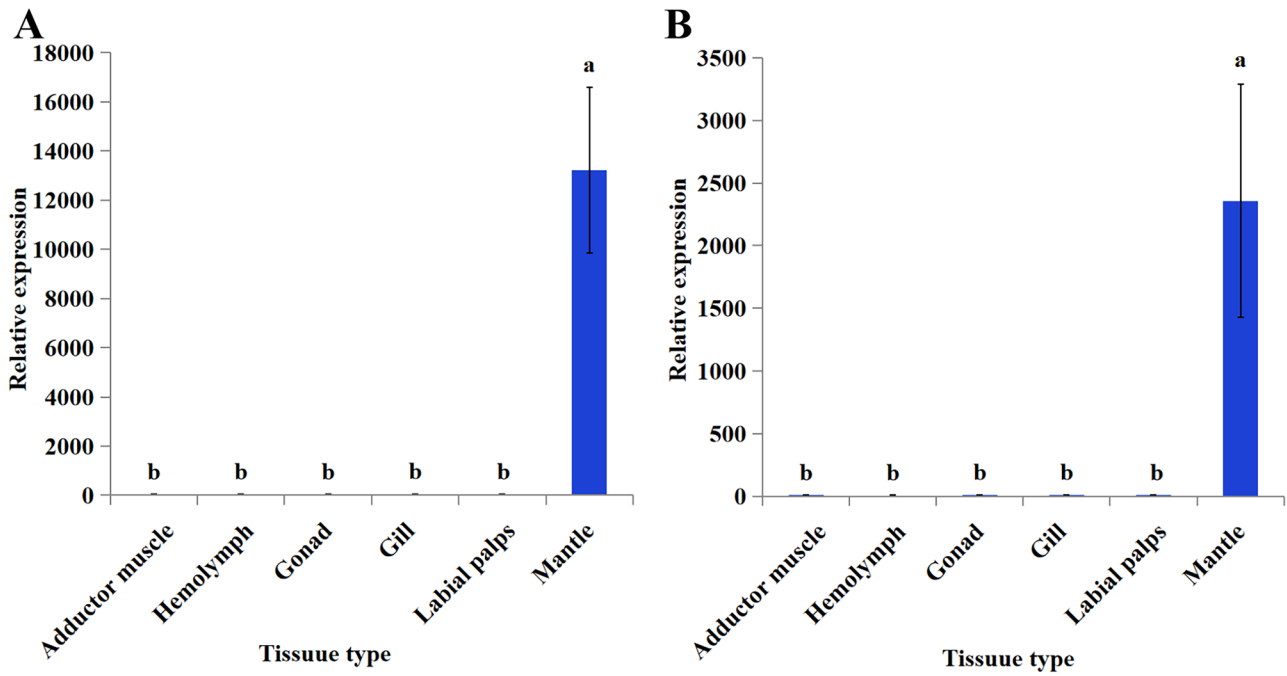
Fig. 3 Tissue expression of *Tyr* (**A**) and *Typ-2* (**B**). The significant difference ($P < 0.05$) among various tissues is indicated by the different lowercase letters

Localization of the Tyrosinases in *C. gigas* During the Embryonic–Larval Developmental Stages

The location of *Typ-2* transcripts was characterized in twelve embryonic–larval developmental stages (Fig. 9). *Typ-2* mRNA was first detected at the trochophore, which was expressed in the whole shell field. In the early D-veliger (18 h), *Typ-2* signals were detected at the edge of the shell field and in the hinge region but not in the central region of the shell field. At a slightly later stage (24 h), *Typ-2* mRNA
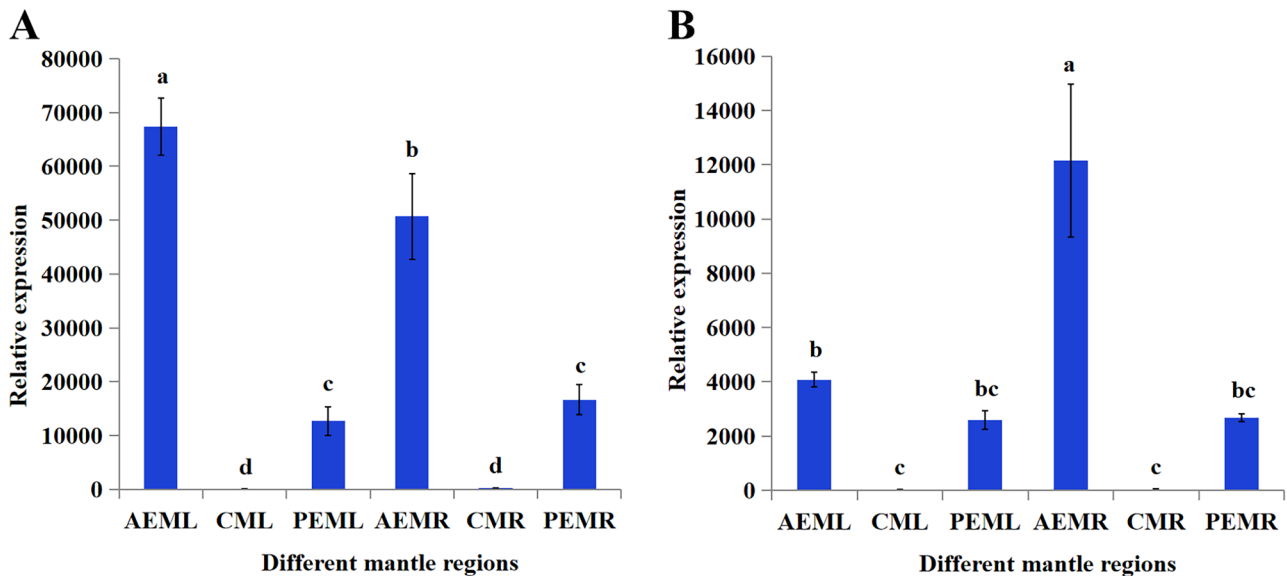

Fig. 4 Relative expression levels of *Tyr* (**A**) and *Typ-2* (**B**) among different mantle regions of *C. gigas*. AEML, anterior side of the left-edge mantle; CML, left-central mantle; PEML, posterior side of the left-edge mantle; AEMR, anterior side of the right-edge mantle; CMR, right-central mantle; PEMR, posterior side of the right-edge mantle. The significant difference ($P < 0.05$) among different mantle regions is indicated by the different lowercase letters
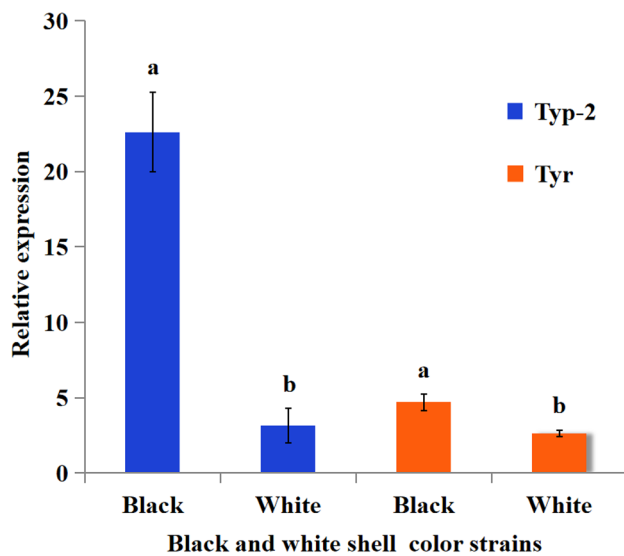
Fig. 5 Relative expression levels of *Tyr* and *Typ-2* between different shell color strains of *C. gigas*. The significant difference ($P < 0.05$) among different shell color strains is indicated by the different lowercase letters

was clearly downregulated and hard to detect. In the subsequently cleavage stages from the umbo-larvae to eyed-larval, the expression of *Typ-2* was continuously not detectable. No positive signal was detected using sense probes (data not shown).

The Tyrosinase Activity in *C. gigas*

The tyrosinase activity in the left-edge and central mantles of the black and white shell colors was shown in Fig. 10. The tyrosinase activity in the edge mantle was significantly higher than that in the central mantle in both shell color oysters, which was generally consistent with the real-time PCR and tissues ISH results. Notably, the tyrosinase activity in the central mantle of the white shell displayed higher levels than that of black shell colors. Though the activity of the edge mantle in the black shell was higher than that in the white shell colors, there was no significant difference between the two shell color oysters.

Discussion

Tyrosinases and tyrosinase-related proteins are members of the type-3 copper protein superfamily. The type-3 copper protein superfamily can be classified into three subclasses based on domain architecture and conserved residues in the copper-binding sites–secreted (a), cytosolic (b), and membrane-bound (c) subclasses (Aguilera et al. 2013). In *C. gigas*, tyrosinase comprises large gene family expansions, leading to paralogues and a number of other duplicates (27 genes total) (Aguilera et al. 2014). In this study, tyrosinase and tyrosinase-like protein 2 named *Tyr* and *Typ-2*, respectively, were identified. The protein sequences of the two
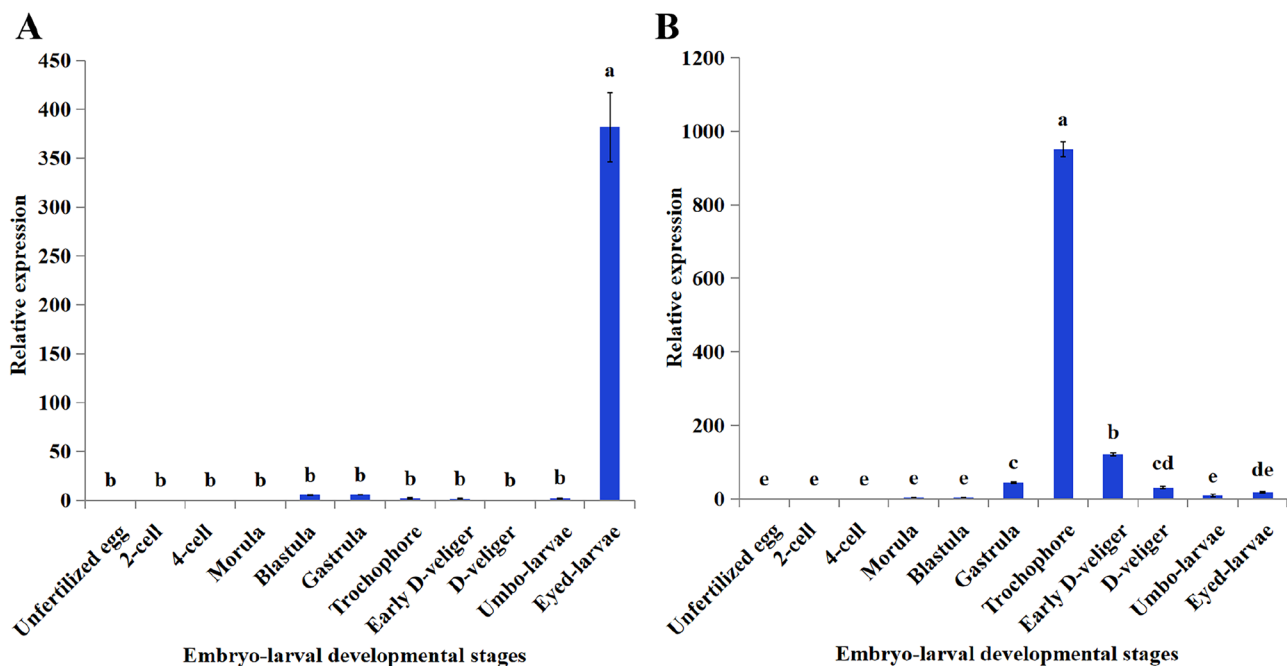

Fig. 6 Relative expression levels of *Tyr* (**A**) and *Typ-2* (**B**) during embryonic and larval stages. The significant difference ($P < 0.05$) among different embryonic–larval developmental stages is indicated by the different lowercase letters

Fig. 7 Tissue distribution of *Tyr* by in situ hybridization. **A** and **B**: Tissue distribution of black shell strains of *C. gigas*. **C** and **D**: Tissue distribution of white shell strains of *C. gigas*. Black arrows indicated the positive signals of *Tyr*. of, outer fold; mf, middle fold; if, inner fold
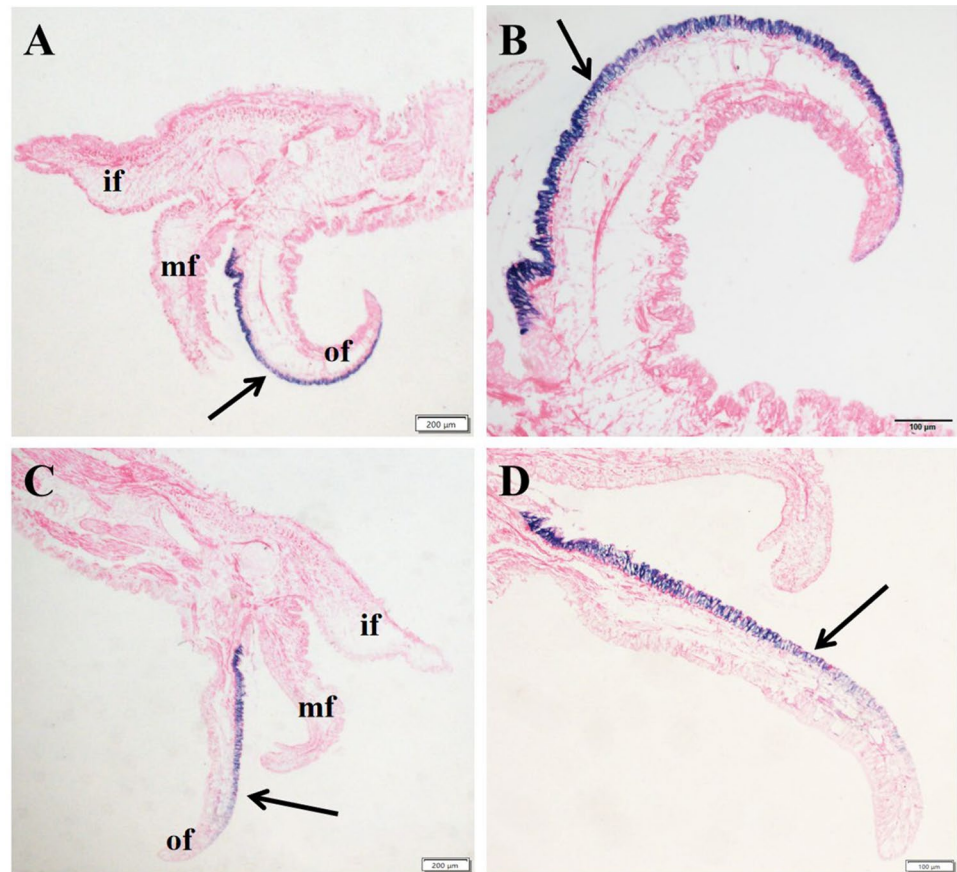
genes contained the important tyrosinase domain with two copper-binding sites of CuA and CuB, supposed to be the sites of catalysis (Chang 2009). The conserved domains of *C. gigas Tyr* and *Typ-2* showed a high degree of similarity with those of other mollusk tyrosinases. This indicated that the two genes belong to the family of tyrosinases, as confirmed by the results of the phylogenetic analysis.

It has been reported that tyrosinase genes played a critical role in various physiological processes, including pigment synthesis, sclerotization of the cuticles, oxygen transport, and innate immunity (Cerenius et al. 2008; Andersen 2010; Cieslak et al. 2011; Chen et al. 2017; Yu et al. 2018). Tissue-specific expression analysis revealed that *Tyr* and *Typ-2* were more highly expressed in the mantle, where they likely contribute to the shell biomineralization and pigmentation (Marin et al. 2012; Lin et al. 2015). The gene expression of *Tyr* and *Typ-2* was mainly restricted to the edge mantle including anterior and posterior mantles, and hardly detectible in the central mantle. In molluscan shells, the deposition of shell layers appears to be controlled by regionalized expression of genes within different zones of the mantle (Jackson et al. 2006, 2007). The molluscan-mantle tissue is usually divided into different zones, distal, central and proximal, with the distal zone in direct contact with the prismatic shell layer and the central and proximal

zones with the nacreous shell layer (Aguilera et al. 2014). Our qPCR results showed high expression of tyrosinase genes in the edge mantle, suggesting the roles in prismatic shell layer construction or periostracum formation. The role of tyrosinase genes in the mantle could also be supported by ISH analysis, in which the *Tyr* and *Typ-2* were mainly expressed at the edge mantle, but not in the central mantle.

Although recent studies have demonstrated that tyrosinase has abundant functions in different cell types (Cerenius et al. 2008; Andersen 2010; Cieslak et al. 2011), the earliest reported function of tyrosinase has an important enzymatic function as one of the phenoloxidases in melanogenesis, which starts with transformation of tyrosine to L-DOPA (Kwon et al. 1988). Here, we found that tyrosinase genes were mainly expressed in the mantle, an organ in direct contact with the shell that is thought to produce shell pigments (Budd et al. 2014). Pigmentation occurs with shell extension and along the growing edge, the position of which continually changes over time as the new shell is added (Williams 2017). The shell pigments of black shell oyster strains are black while white shell oyster strains are non-pigmentation (Fig. 1). Considering the occurrence of shell color in oysters is associated with gene expression changes, it is critical to determine how genes regulate pigmentation in oysters. The reported pigmentation-involved function of tyrosinase genes

Fig. 8 Tissue distribution of *Typ-2* by in situ hybridization. **A** and **B**: Tissue distribution of black shell strains of *C. gigas*. **C** and **D**: Tissue distribution of white shell strains of *C. gigas*. Black arrows indicated the positive signals of *Typ-2*. of, outer fold; mf, middle fold; if, inner fold
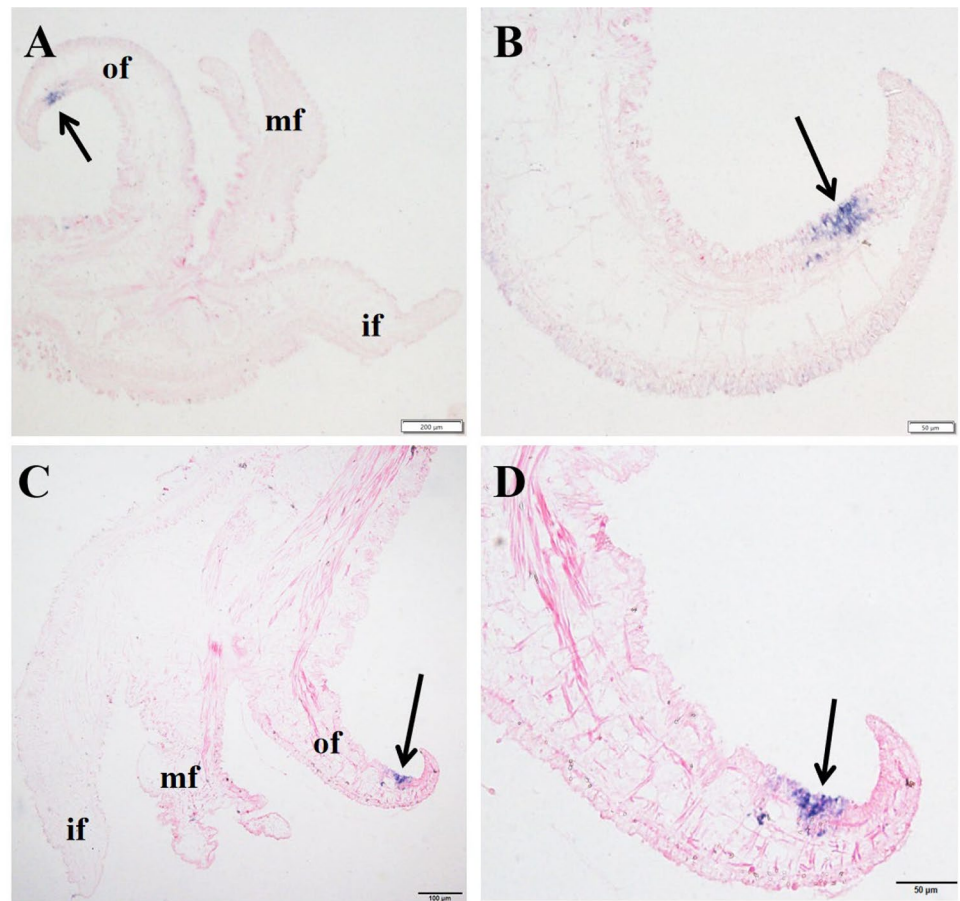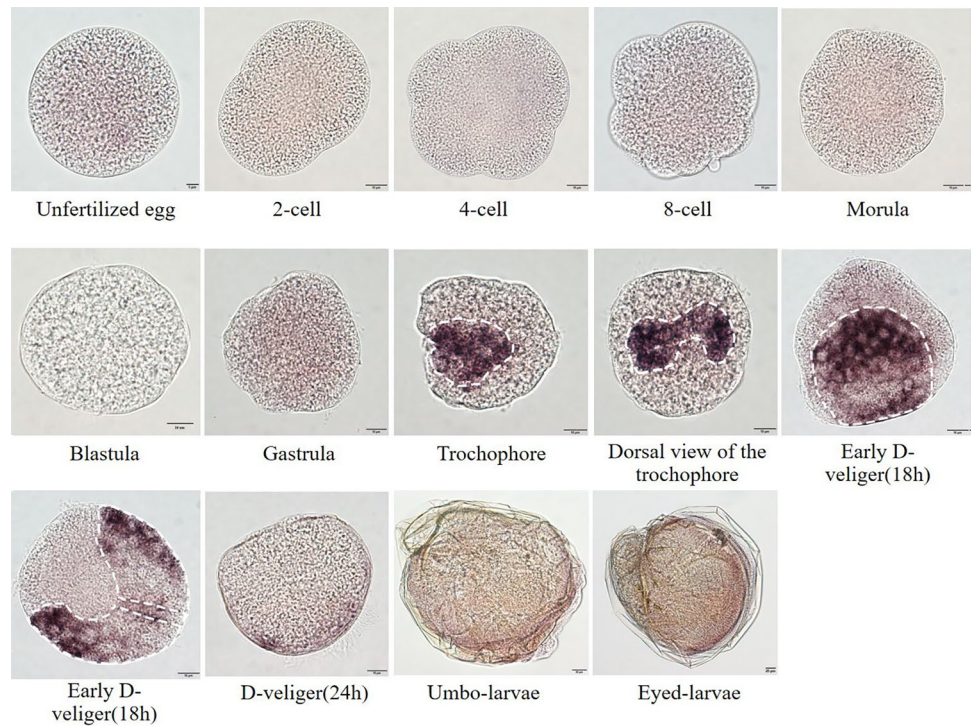

Fig. 9 Distribution of *Typ-2* during embryonic and larval stages by whole mount in situ hybridization. The white dotted lines indicated the shell field and the shell hinges were indicated by double lines
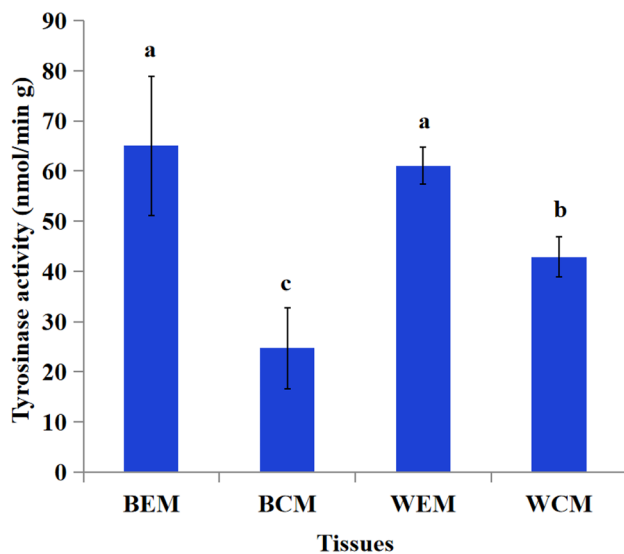

Unfertilized egg   2-cell   4-cell   8-cell   Morula

Blastula   Gastrula   Trochophore   Dorsal view of the trochophore   Early D-veliger(18h)

Early D-veliger(18h)   D-veliger(24h)   Umbo-larvae   Eyed-larvae

Fig. 10 The tyrosinase activity in the different mantle regions of the left side of black and white shell strains of *C. gigas*. BEM, edge mantle of black shell colors; BCM, central mantle of black shell colors; WEM, edge mantle of white shell colors; WCM, central mantle of white shell colors. The significant difference ($P < 0.05$) among different mantle regions of the left side is indicated by the different lowercase letters

and the high expression of *Tyr* and *Typ-2* in the black shell confirmed the important role of the two genes in the shell pigmentation of *C. gigas*. Similarly, knockdown *P. penguin PpTyr* significantly decreased the formation of melanin, indicating that tyrosinase was a determinant of melanin synthesis in *P. penguin* (Yu et al. 2018). Knockdown of both zebrafish *Tyrp1* genes resulted in the formation of brown instead of black eumelanin accompanied by severe melanosome defects, suggesting that black eumelanin formation essentially relies on the presence of *Tyrp1* (Braasch et al. 2009). In mollusca, the mantle involves in the calcification of varieties of macromolecular protein, secretion of matrix proteins, and other secreted factors, which promote shell deposition (Song et al. 2019). Indeed *Tyr* and *Typ-2* were expressed at the outer fold of the edge mantle. This further highlighted the potential roles of tyrosinase-related genes in pigmentation. Interestingly, *Tyr* was mainly localized in the epithelial cells of the inner surface of the outer fold, while *Typ-2* signals were detected in the epithelial cells of the outer surface of the outer fold. In all bivalves, the periostracum arises from a groove located between the outer fold and the middle fold (Jabbour-Zahab et al. 1992). The epithelial layer in the inner surface of the outer fold, composed of cells with microvilli, which may play an important part in periostracum maturation through the secretion of neutral glycoproteins (Jabbour-Zahab et al. 1992). In general, it is demonstrated that eumelanin mainly occurs in the outermost, non-mineralized and highly pigmented layer of

the shell (referred to as the periostracum) (Affenzelle et al. 2019). These observations potentially revealed that *Tyr* gene may be involved in the shell coloration in oysters. On the other hand, the prismatic layer of the shell is derived exclusively from the tall columnar cells lining the outer surface of the outer mantle fold. Some studies revealed that the middle layer of the periostracum was involved in the prismatic layer of the shell (Jabbour-Zahab et al. 1992; Checa et al. 2012). Based on these, we speculate that the *C. gigas Typ-2* is more likely to play critical roles not only in the formation of the prismatic layer of the shell but also in shell pigmentation in adult oysters as demonstrated in *H. cumingii* (Chen et al. 2017).

Tyrosinase activity is found both in the particulate and soluble fractions of the cells (Iwata et al. 1990). In this study, the edge mantle demonstrated higher levels of tyrosinase activity than that in the central mantle in the two strains of *C. gigas*, suggesting its potential function in the formation of periostracum and prismatic shell layer. In addition, the edge-mantle activity of black shell was higher than that in the white shell colors. The black-pigmented tissues may have higher enzyme activity, as the amount of melanin synthesis was positively correlated with the activity of tyrosinase (Jackson and Bennett 1990). Tyrosinase proteins were found in the prismatic shell layer of *P. fucata*; this layer is recognized as the pigmented region in *P. fucata* (Nagai et al. 2007). The spatial localization of tyrosinase in the pigmented shell and mantle tissue suggests a role in shell pigmentation (Nagai et al. 2007). Surprisingly, the tyrosinase activity in the central mantle of the white shell was significantly higher than that in the black shell colors. In *Haliotis asinina*, pigments were localized in the edge mantle, implying the important role of this mantle zone in shell pigmentation (Budd et al. 2014), but whether the central mantle functions in shell color formation is still unclear. The differences in tyrosinase activity in the central mantle among different shell colors may be due, not only to different numbers of enzymes but also possibly to different catalytic activity of enzyme (Iwata et al. 1990).

To better understand the role of tyrosinase genes in the early embryonic development, the expression patterns were examined during ontogenesis in the black shell *C. gigas*. Expression pattern analysis indicated that high expression level of *Tyr* was detected in eyed-larvae. It was reported that, the eyes in oysters developed in the larva only during the eyed-larvae which were a pair of spherical densely pigmented organs, situated in the body wall just dorsal to the attachment of the gill rudiments (Cole and Sc 1938). Each eyespot consists of an almost spherical cup of pigmented epithelium, which distributes large amounts of pigmented granules (Cole and Sc 1938). Based on these observations, it is suggested that *Tyr* plays a key role in pigmentation of *C. gigas*. This phenomenon

has also been observed in *Siniperca chuatsi* (Wu et al. 2020) and zebrafish (Camp and Lardelli 2001). Besides, the *tyr* mRNA expression level also changed correspondingly with their body pigmentation in the different embryonic development stages. In contrast, *Typ-2* was highly expressed in the trochophore stage, which represents the time of initial non-calcified shell (InCaS) formation, suggesting that *Typ-2* might be involved in InCaS formation. The *Typ-2* maintained higher expression level until the early D-veliger (18 h) stage, then dramatically downregulated at D-veliger (24 h) and was hardly detected at the umbo-larvae and eyed-larvae stages. ISH indicated that *Typ-2* mRNA was distributed in the whole shell field at the trochophore stage, and detected in the edge of the shell field and hinge region at the early D-veliger (18 h) stage. Tyrosinase 1 in normal *C. gigas* also showed the similar patterns (Huan et al. 2013). Differently, the cells at the edge of the shell field and in the hinge region expressed *cgi-tyr1* at about 14 h. The difference may be due to the bias of incubation temperature during embryonic development. The InCaS was first formed during the trochophore stage (Moueza et al. 2006), suggesting that *Typ-2* may function in the biogenesis of the larval shell. A recent study also reported that *tyrA1* might participate in the biogenesis of the initial non-calcified shell of trochophores in *Crassostrea angulata* (Yang et al. 2017).

In summary, we identified and characterized two tyrosinase genes in *C. gigas*; phylogenetic and sequence feature analyses confirmed their identities and evolutionary status. Most importantly, expression patterns of tyrosinase genes in different mantle regions and different shell colors proved an important role in shell biosynthesis and pigmentation. In particular, *Typ-2* gene was involved in the initial non-calcified shell of trochophores. The work provides valuable information for the molecular mechanism study of shell formation and pigmentation in the Pacific oyster.

Declarations

References

Affenzelle S, Wolkenstein K, Frauendorf H, Jackson DJ (2019) Eumelanin and pheomelanin pigmentation in mollusc shells may be less common than expected: insights from mass spectrometry. Front Zool 16:47

Aguilera F, McDougall C, Degnan BM (2013) Origin, evolution and classification of type-3 copper proteins: lineage-specific gene expansions and losses across the Metazoa. BMC Evol Biol 13:96

Aguilera F, McDougall C, Degnan BM (2014) Evolution of the tyrosinase gene family in bivalve molluscs: independent expansion of the mantle gene repertoire. Acta Biomater 10:3855–3865

Alfnes F, Guttormsen AG, Steine G, Kolstad K (2006) Consumers' willingness to pay for the color of salmon: a choice experiment with real economic incentives. Am J Agric Econ 88:1050–1061

Andersen SO (2010) Insect cuticular sclerotization: a review. Insect Biochem Mol Biol 40:166–178

Bai G, Brown JF, Watson C, Yoshino TP (1997) Isolation and characterization of phenoloxidase from egg masses of the gastropod mollusc, *Biomphalaria glabrata*. Comp Biochem Physiol B Biochem Mol Biol 118:463–469

Budd A, McDougall C, Green K, Degnan BM (2014) Control of shell pigmentation by secretory tubules in the abalone mantle. Front Zool 11:62

Braasch I, Liedtke D, Volff JN, Schartl M (2009) Pigmentary function and evolution of tyrp1 gene duplicates in fish. Pigment Cell Melanoma Res 22:839–850

Camp E, Lardelli M (2001) Tyrosinase gene expression in zebrafish embryos. Dev Genes Evol 211:150–153

Cerenius L, Lee BL, Söderhäll K (2008) The proPO-system: pros and cons for its role in invertebrate immunity. Trends Immunol 29:263–271

Chang TS (2009) An updated review of tyrosinase inhibitors. Int J Mol Sci 10:2440–2475

Checa A, Harper EM, Willinger M (2012) Aragonitic dendritic prismatic shell microstructure in *Thracia* (Bivalvia, Anomalodesmata). Invertebr Biol 131:19–29

Chen X, Liu X, Bai Z, Zhao L, Li J (2017) HcTyr and HcTyp-1 of *Hyriopsis cumingii*, novel tyrosinase and tyrosinase-related protein genes involved in nacre color formation. Comp Biochem Physiol B Biochem Mol Biol 204:1–8

Cieslak M, Reissmann M, Hofreiter M, Ludwig A (2011) Colours of domestication. Biol Rev Camb Philos Soc 86:885–899

Cole HA, Sc M (1938) The fate of the larval organs in the metamorphosis of *Ostrea edulis*. J Mar Biol Assoc U K 22:469–484

Feng D, Li Q, Yu H (2019) RNA interference by ingested dsRNA-expressing bacteria to study shell biosynthesis and pigmentation in *Crassostrea gigas*. Mar Biotechnol 21:526–536

Feng D, Li Q, Yu H, Zhao X, Kong L (2015) Comparative transcriptome analysis of the Pacific oyster *Crassostrea gigas* characterized by shell colors: identification of genetic bases potentially involved in pigmentation. PLoS One 10:e0145257

Gutierrez-Gil B, Wiener P, Williams JL (2007) Genetic effects on coat colour in cattle: dilution of eumelanin and phaeomelanin pigments in an F2-backcross Charolais × Holstein population. BMC Genet 8:56–67

Han Z, Li Q (2020) Mendelian inheritance of orange shell color in the Pacific oyster *Crassostrea gigas*. Aquac 516:734616

Hoekstra HE (2006) Genetics, development and evolution of adaptive pigmentation in vertebrates. Heredity 97:222–234

Huan P, Liu G, Wang H, Liu B (2013) Identification of a tyrosinase gene potentially involved in early larval shell biogenesis of the Pacific oyster *Crassostrea gigas*. Dev Genes Evol 223:389–394

Iwata M, Corn T, Iwata S, Everett MA, Fuller BB (1990) The relationship between tyrosinase activity and skin color in human foreskins. J Invest Dermatol 95:9–15

Jabbour-Zahab R, Chagot D, Blanc F, Grizel H (1992) Mantle histology, histochemistry and ultrastructure of the pearl oyster *Pinctada margaritifera* (L.). Aquat Living Res 5:287–298

Jackson DJ, McDougall C, Green K, Simpson F, Wörheide G, Degnan BM (2006) A rapidly evolving secretome builds and patterns a sea shell. BMC Biol 4:40

Jackson DJ, Worheide G, Degnan BM (2007) Dynamic expression of ancient and novel molluscan shell genes during ecological transitions. BMC Evol Biol 7:160

Jackson IJ, Bennett DC (1990) Identification of the albino mutation of mouse tyrosinase by analysis of an in vitro revertant. Proc Natl Acad Sci U S A 87:7010–7014

Kumar S, Stecher G, Tamura K (2016) MEGA7: molecular evolutionary genetics analysis version 7.0 for bigger datasets. Mol Biol Evol 33:1870–1874

Kwon BS, Wakulchik M, Haq AK, Halaban R, Kestler D (1988) Sequence analysis of mouse tyrosinase cDNA and the effect of melanotropin on its gene expression. Biochem Biophys Res Commun 153:1301–1309

Lemer S, Saulnier D, Gueguen Y, Planes S (2015) Identification of genes associated with shell color in the black-lipped pearl oyster, *Pinctada Margaritifera*. BMC Genom 16:568

Letunic I, Doerks T, Bork P (2015) SMART: recent updates, new developments and status in 2015. Nucleic Acids Res 43:D257–D260

Lin C, Yang C, Lin Y, Chiu Y, Chen C (2015) Establishment of a melanogenesis regulation assay system using a fluorescent protein reporter combined with the promoters for the melanogenesis-related genes in human melanoma cells. Enzym Microb Technol 68:1–9

Liu X, Wu F, Zhao H, Zang G, Guo X (2009) A novel shell color variant of the Pacific abalone *Haliotis discus hannai* Ino subject to genetic control and dietary influence. J Shellfish Res 28:419–424

Luna-González A, Maeda-Martínez AN, Vargas-Albores F, Ascencio-Valle F, Robles-Mungaray M (2003) Phenoloxidase activity in larval and juvenile homogenates and adult plasma and haemocytes of bivalve molluscs. Fish Shellfish Immunol 15:275–282

Marin F, Le Roy N, Marie B (2012) The formation and mineralization of mollusk shell. Front Biosci 4:1099–1125

McDougall C, Degnan BM (2018) The evolution of mollusc shells. Wiley Interdiscip Rev Dev Biol 7:e313

Moueza M, Gros O, Frenkiel L (2006) Embryonic development and shell differentiation in *Chione cancellata* (Bivalvia, Veneridae): an ultrastructural analysis. Inverteb Biol 125:21–33

Nagai K, Yano M, Morimoto K, Miyamoto H (2007) Tyrosinase localization in mollusc shells. Comp Biochem Physiol B Biochem Mol Biol 146:207–214

Palumbo A (2003) Melanogenesis in the ink gland of *Sepia officinalis*. Pigm Cell Res 16:517–522

Ren G, Chen C, Jin Y, Zhang G, Hu Y, Shen W (2020) A novel tyrosinase gene plays a potential role in modification the shell organic matrix of the triangle mussel *Hyriopsis cumingii*. Front Physiol 11:100

Song X, Liu Z, Wang L, Song L (2019) Recent advances of shell matrix proteins and cellular orchestration in marine molluscan shell biomineralization. Front Mar Sci 6:41

Takgi R, Miyashita T (2014) A cDNA cloning of a novel alpha-class tyrosinase of *Pinctada fucata*: its expression analysis and characterization of the expressed protein. Enzym Res 2014:1–9

Wang Q, Li Q, Kong L, Yu R (2012) Response to selection for fast growth in the second generation of Pacific oyster (*Crassostrea gigas*). J Ocean Univ China 11:413–418

Williams ST (2017) Molluscan shell colour. Biol Rev 92:1039–1058

Williams ST, Lockyer AE, Dyal P, Nakano P, Churchill CKC, Speiser DI (2017) Colorful seashells: identification of haem pathway genes associated with the synthesis of porphyrin shell color in marine snails. Ecol Evol 7:10379–10397

Wu M, Chen X, Cui K, Li H, Jiang Y (2020) Pigmentation formation and expression analysis of tyrosinase in *Siniperca chuatsi*. Fish Physiol Biochem 46:1279–1293

Xu C, Li Q, Yu H, Liu S, Kong L, Chong J (2019) Inheritance of shell pigmentation in Pacific oyster *Crassostrea gigas*. Aquac 512:734249

Xu R, Li Q, Yu H, Kong L (2018) Oocyte maturation and origin of the germline as revealed by the expression of nanos-like in the Pacific oyster *Crassostrea gigas*. Gene 663:41–50

Yang B, Pu F, Li L, You W, Ke C, Feng D (2017) Functional analysis of a tyrosinase gene involved in early larval shell biogenesis in *Crassostrea angulata* and its response to ocean acidification. Comp Biochem Physiol B Biochem Mol Biol 206:8–15

Yu F, Pan Z, Qu B, Yu X, Xu K, Deng Y, Liang F (2018) Identification of a tyrosinase gene and its functional analysis in melanin synthesis of *Pteria penguin*. Gene 656:1–8

Yu H, Zhao X, Li Q (2016) Genome-wide identification and characterization of long intergenic noncoding RNAs and their potential association with larval development in the Pacific oyster. Sci Rep 6:20796

Yusa Y (2004) Inheritance of colour polymorphism and the pattern of sperm competition in the apple snail *Pomacea canaliculata* (Gastropoda: Ampullariidae). J Molluscan Stud 70:43–48

Zhu Y, Li Q, Yu H, Kong L (2018) Biochemical composition and nutritional value of different shell color strains of Pacific oyster *Crassostrea gigas*. J Ocean Univ China 17:897–904